

PRESSURE WALL MEASUREMENTS IN THE WHOLE DRAFT TUBE: STEADY AND UNSTEADY ANALYSIS

Jorge ARPE,

*Swiss Federal Institute of Technology/LMH,
Lausanne, Switzerland*

François AVELLAN,

ABSTRACT

Flow in a elbow draft tube is a turbulent complex unsteady flow caused by its rotating nature and the draft tube's geometry. The understanding of the main phenomena that could appear near the BEP and at off-design conditions is important to master the instability of the machine. The results shown in this work are a summary of a very large experimental database. The aim of this investigation work is to analyze the steady and unsteady pressure fields at the wall of the draft tube through extensive pressure measurements. A particular evolution of the steady pressure field appeared according to the operating points around the BEP chosen to study the draft tube recovery break-off. Consequently, the flow is distributed between the 2 channels of the draft tube according to the operating point. The fluctuating pressure field at the cone can be divided mainly in 2 components: first a rotating component at the runner's frequency (f^*) and second a synchronous component at $20f^*$ resultant of the interaction rotor-stator frequency. The influence of the spiral casing on the fluctuating pressure is pointed out by representing all phase average signals in the same absolute angular position of the runner. The results at the low discharge operating point without vapour phase show the main pressure fluctuations at the cavitation free vortex frequency as well as the advection of these fluctuations in the elbow and the channel walls.

RÉSUMÉ

L'écoulement dans un diffuseur coudé de turbine est complexe, instationnaire et turbulent, en raison de sa nature tournante et de la géométrie du diffuseur. La compréhension des phénomènes qui peuvent apparaître aux points de fonctionnement dits 'tranquilles', c'est-à-dire autour du point optimal, et aux points de fonctionnement "off-design", sont importants pour la prédiction et la maîtrise de l'instabilité de la machine. Les résultats montrés dans ce travail de recherche représentent une partie d'une très importante base de données expérimentale. Le but de ce travail est d'analyser les champs de pression stationnaires et non stationnaires aux parois du diffuseur à travers des mesures de pression systématiques. Une évolution particulière du champ de pression stationnaire est mise en évidence selon les points de fonctionnement autour du point optimal choisis pour étudier la chute du coefficient de récupération de pression du diffuseur. Comme résultat il s'ensuit une distribution du débit entre les 2 canaux du diffuseur selon le point de fonctionnement. Le champ fluctuant dans le cône montre principalement 2 composantes: une composante tournante à la fréquence de rotation de la roue (f^*) et une composante synchrone à $20f^*$ résultant de l'interaction rotor-stator. L'influence du bec de bêche sur les fluctuations de pression est mise en évidence en représentant tous les signaux de moyennes de phase selon la position angulaire absolue de la roue. Les résultats à débit partiel sans phase vapeur montrent les principales fluctuations à la fréquence de la torche et les mouvements de ces fluctuations aux parois dans le coude et les canaux.

NOMENCLATURE

| Term | Symbol | Definition | Term | Symbol | Definition |
|---------------------------|--------|------------|------------------------|----------|------------|
| Flow Velocity | C | m/s | Runner Outlet Diameter | D | m |
| Specific Hydraulic Energy | E | gH | Angular Speed | ω | rad^{-1} |
| Net Head | H | m | Discharge | Q | m^3/s |

| Term | Symbol | Definition | Term | Symbol | Definition |
|---------------------------------|--------|--|------------------------------|-------------|----------------------------|
| Static Pressure | p | Pa | Fluctuating Static Pressure | \tilde{p} | Pa |
| Specific Energy Coefficient | ψ | $2E / (\omega D / 2)^2$ | Discharge Coefficient | φ | $Q / \pi \omega (D / 2)^3$ |
| Pressure Coefficient | C_p | $\frac{p - p_{ref}}{\frac{1}{2} \rho C_{ref}^2}$ | Thoma Number | σ | $NPSE / E$ |
| Best Efficiency Point | BEP | | Net Specific Positive Energy | $NPSE$ | |
| Inlet Section of the Draft Tube | ref | | Non dimensional frequency | f^* | f / f_n |

INTRODUCTION

The flow analysis of the draft tube of an hydraulic turbine is of practical interests for either the design of new machines or the rehabilitation of existing ones. The specific pressure energy recovery in the draft tube affects significantly the efficiency and power output of the machines at high discharge (Ref. 1). The bad prediction of the flow could lead to have unexpected efficiency break-off similar as Fig. 1. Also, the hydraulic turbines which operate under a wide range of heads and outputs, are subjected to considerable pulsating pressures at off design conditions produced by a vortex rope in the draft tube that could lead to pressure surges in the hydraulic system. Many works to suppress or alleviate these pressure fluctuations at low discharge were studied (Refs. 4, 5). We can found also studies about the characterization of the vortex rope and modeling (Refs. 6, 7). In these work we will contribute to the knowledge of these phenomena in studying the steady and unsteady pressure field obtain by an extensive pressure measurements at the whole draft tube.

In the FLINDT frame work, we will present 2 cases. The first case concerns the analysis of pressure measurements at the operating points close to the BEP to explain the draft tube pressure recovery break-off observed at the Fig. 1. The break-off numerical analysis proposed by Mauri (Ref. 2) at the same conditions, leads to a bifurcation of the flow rate due to a Werlé-Legendre vortex which appears at the right channel. The size and strength of this vortex increase with the discharge, leading to an obstruction of the right channel and to an increase of the draft tube global losses. This is the basis to explain the evolution of the steady pressure field.

The second case concerns the analysis of measurements of the operating point at low discharge. Even though the periodic nature of the fluctuations and its frequency produced by the rope is well known, the analysis of signals in the whole draft tube allows to follow these fluctuations and a good description of the rope behaviour through sections. Mauri (Ref. 2) also performed a calculation at low discharge without vapor phase with similar conditions. These calculations show a fast decrease of the fluctuations magnitude at the elbow already. In any case, they are a very useful tool to start the experimental analysis and measurements will be able to qualify the reliability of these computations.

EXPERIMENTAL DETAILS

The investigated model is a Francis turbine described in Avellan (Ref. 1). To perform the pressure measurements, the draft tube is equipped with 292 taps, see Fig. 3. A set of Keller Piezoresistive Pressure Transducers series 2MI is used. The signal acquisition is performed simultaneously on 104 channels with a HP-VXI system, see Fig. 4. An optical encoder is used to synchronize the measurements and the runner position in order to perform the phase average analysis for all signals in the draft tube. 3 ranges of frequencies is analysed: in the low frequencies, 200 Hz - 2^{14} samples, medium frequencies, 1'280 Hz - 2^{15} samples, and high frequencies from 6 kHz - 2^{16} samples. The measurements are made non dimensionnall by the specific kinetic energy at the inlet of the draft tube.

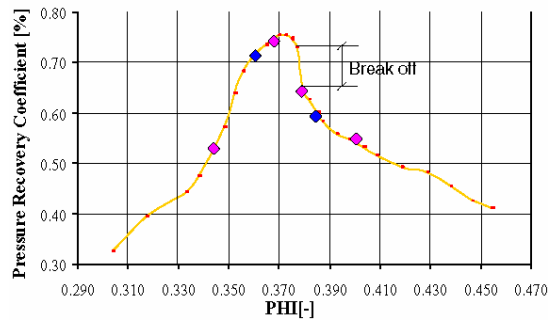


Fig. 1 Recovery Hill Chart

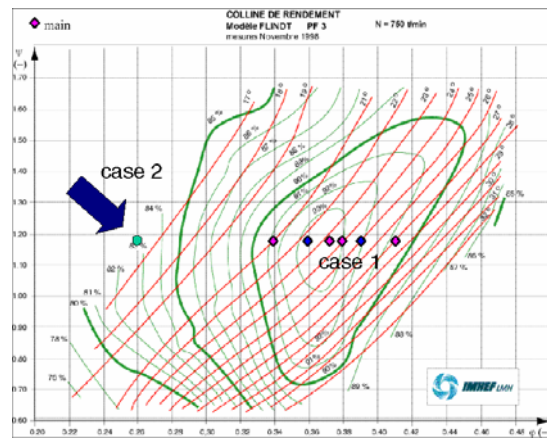


Fig. 2 Studied Operating Points

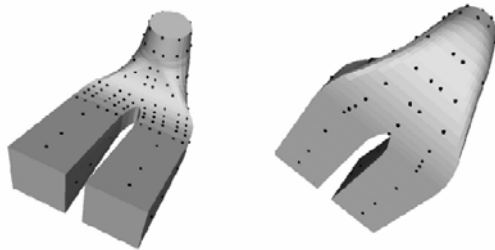


Fig. 3 Pressure taps in the draft tube

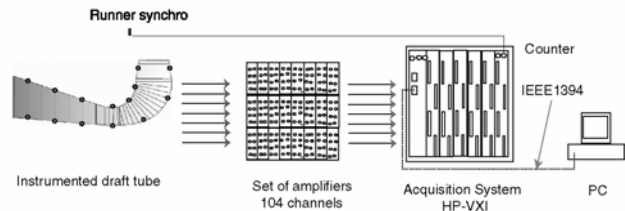


Fig. 4 Wall pressure instrumentation

For the visualization of the results, the draft tube walls are unfolded on a plan. The transducers positions are represented according to Fig. 5. Each node corresponds to a sensor position.

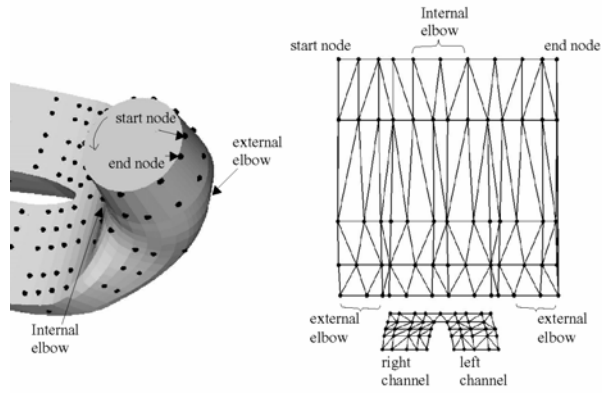
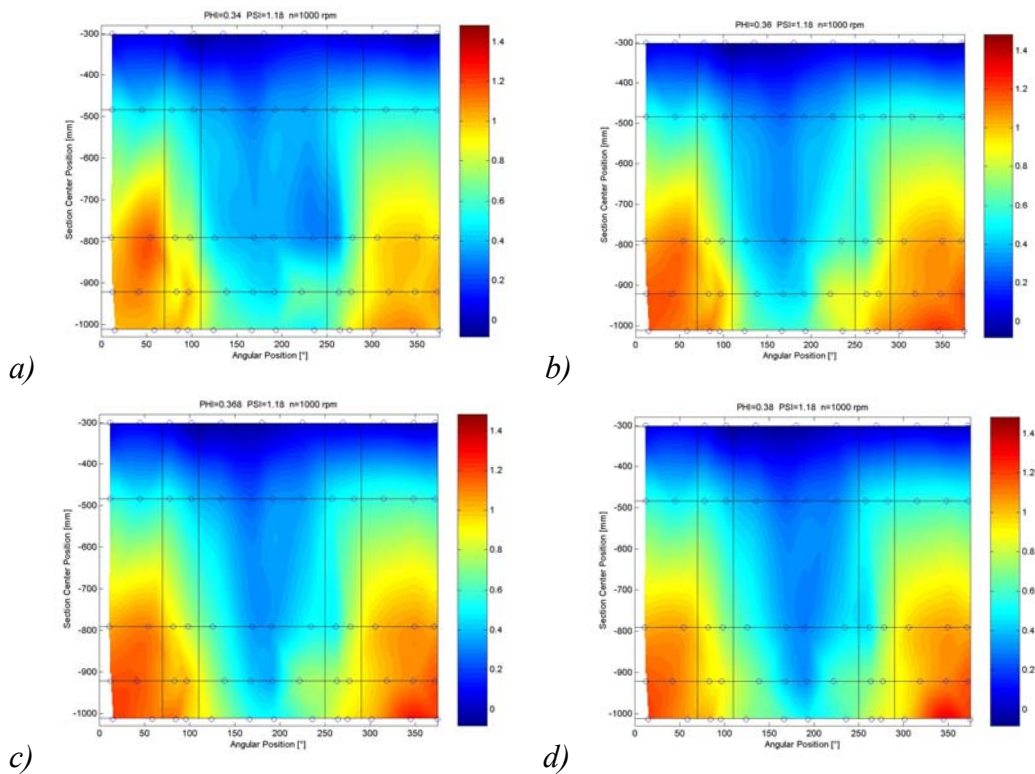


Fig. 5 Representation of the unfolded draft tube and the sensors

CASE 1: ANALYSIS ON THE BREAK-OFF PRESSURE RECOVERY

The steady analysis of the measurements performed at the operating points according to Fig. 1, allow us to visualize the evolution of the static pressure coefficient C_p as a function of the discharge. In the Fig. 6(a-f) we can observe the steady field pressure in the cone and in the elbow. Fig. 7(a-f) shows the evolution of the steady field pressure in the channels inlet (top and bottom). These pictures show very clearly a particular behaviour at the wall. The zones where the pressure is lowest in the internal elbow are also the zones with the highest local flow velocity. For the operating point at lowest discharge, there is a tendency of the flow to turn to the left channel, see Fig. 6a and Fig. 7a. At the next operating point, the flow turns suddenly towards the right channel, see Fig. 6b and Fig. 7b, and we observe that the flow is significantly different than in the previous case. For the next operating points, see Fig. 6c-6f and Fig. 7c-7f, the flow turns to the left channel and the flow rate increases progressively in that channel. We conclude that highest velocities can be found in the left channel. At the bottom of the pier, see Fig. 7(a-f), we observe that the static pressure around the pier increases with the flow rate. The point of maximum pressure value corresponds to the stagnation point. The behaviour that we described above is consistent with Mauri's conclusions (Ref. 2), who observed the same increases of the flow rate in the left channel as a result of the obstruction of the right channel by a separation vortex.



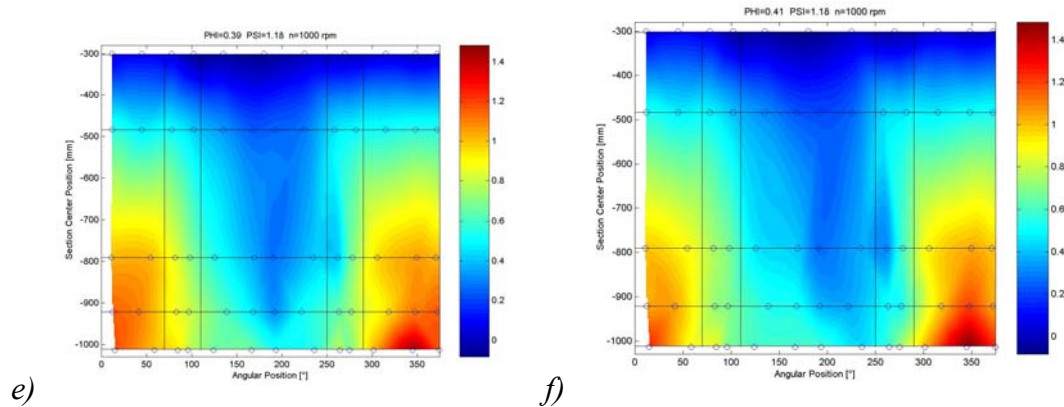


Fig. 6 Evolution of the static pressure field in the cone and elbow

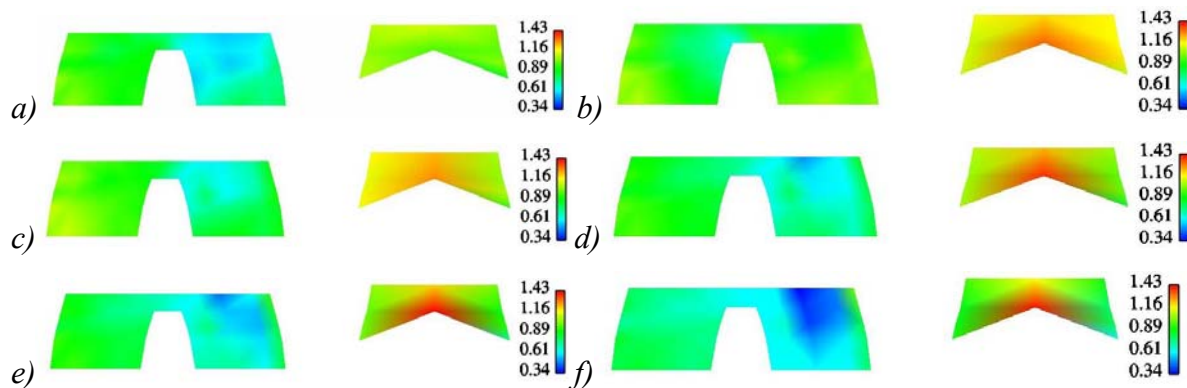


Fig. 7 Evolution of the static pressure field in the channels (top and bottom)

Unsteady analysis in the cone

Sections S1.3 and S1.75 are studied in the cone, Fig. 9. The amplitude spectral analysis points out the main characteristic frequencies, see Fig. 8, as the runner's rotating frequency (f^*), its harmonics, the interaction rotor-stator frequency ($20f^*$) and the blades passage frequency ($17f^*$) whose amplitude appears slightly. Fig. 9 represents the results of the average pressure fluctuations in the polar representation. In the section S1.3, the fluctuations at the runner frequency have a phase shift according to the angular position of the sensors. This is the fluctuating rotating component. The fluctuations at $20f^*$ is the result of the interaction between the runner and the 20 guide vanes. They are in phase and represent the fluctuating synchronous component. In the section S1.75 a particular behavior can be observed: the fluctuations at the runner and blade passage frequency decrease significantly and only the synchronous fluctuation at $20f^*$ is visible.

Fig. 10 represents the phase averaged pressure fluctuations reported to the absolute position of the runner over one period. The minimum of the fluctuations corresponds to the tongue position in the spiral casing. It shows the participation of the tongue in the modulation perturbation of the pressure fluctuation field. Signals are not in phase because the phase shift of the fluctuations at the runner frequency does not exactly correspond with the geometrical position of the sensors in the section, see Fig. 11. This could be explained by the elbow's influence on the fluctuations.

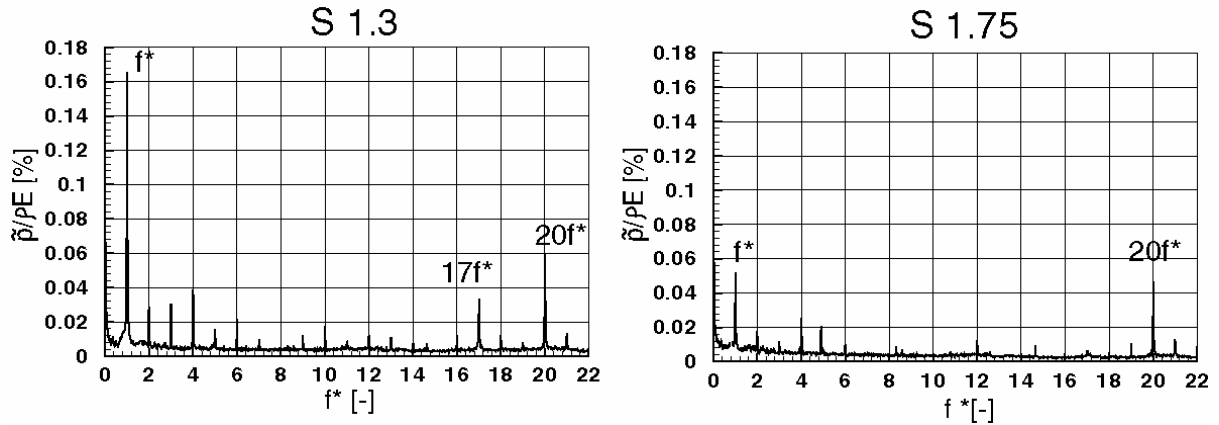


Fig. 8 Amplitude spectrum in the cone

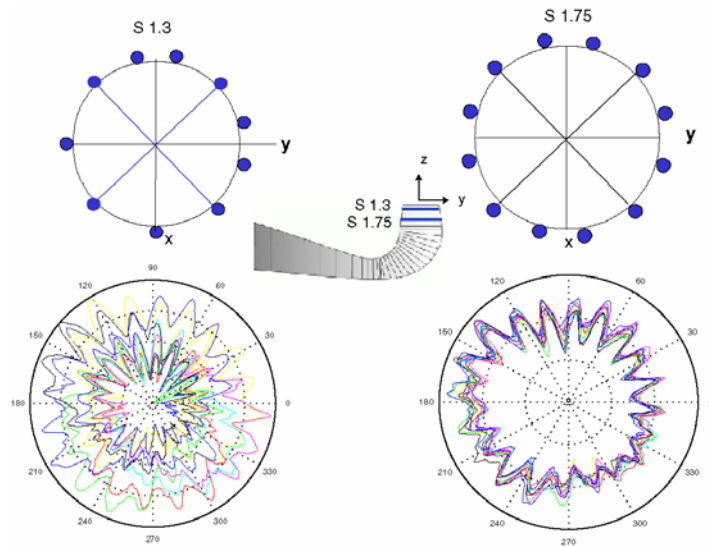


Fig. 9 Phase average results in the cone in a polar representation

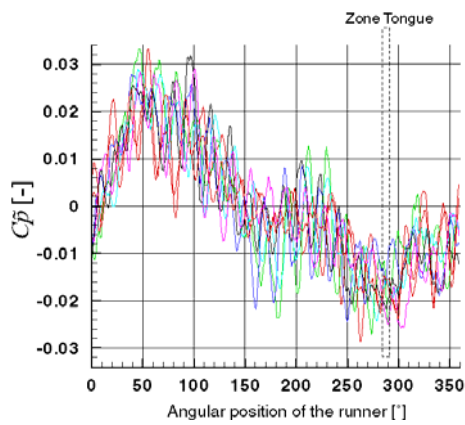


Fig. 10 Phase average reported to the absolute

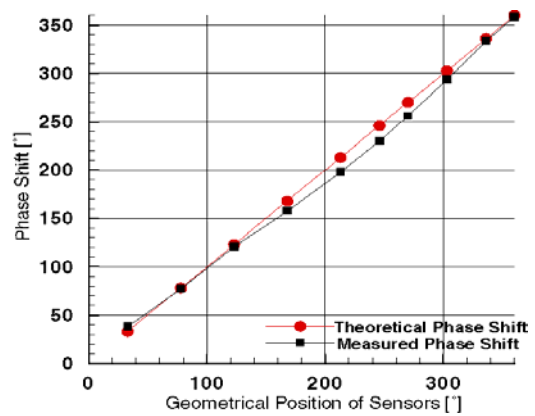


Fig. 11 Phase shift between signals in S1.3 runner position

CASE 2: LOW DISCHARGE OPERATING POINT ANALYSIS

In this section is presented part of the results obtained at low discharge measurements at $\psi = 1.18$, $\varphi = 0.26$, $n = 750\text{t/min}$, opening 16° , $\sigma = 1.18$ with no vapor phase, see Fig. 2. The measurements are triggered with the vortex passage to synchronize them and perform the unsteady analysis.

The results of the phase average at the vortex frequency are illustrated in Fig. 12. They correspond to the 5 first sections of the draft tube according to a generating line across the draft tube, from top to bottom. High periodicity of the signals for 3 vortex passages is observed. At the left of this figure are represented the pressure fluctuation fields for a given phase obtained by Mauri's calculations. The shapes of the fluctuations can be explained as follows: at the section S1.3 the fluctuations have a sinusoidal shape, the vortex core, low pressure zone, turns close the axis of the machine, the minimum of the fluctuations occurs when the rope core passes close the sensor. At the section S1.75 the vortex core turns around the axis of the machine but close the cone wall and the fluctuations amplitude increases. There is a very fast drop in the fluctuations due to a brief passage of the vortex core. In the next sections the amplitude of the fluctuations decreases progressively. The phase shift between the signals is observed also in the numerical calculation.

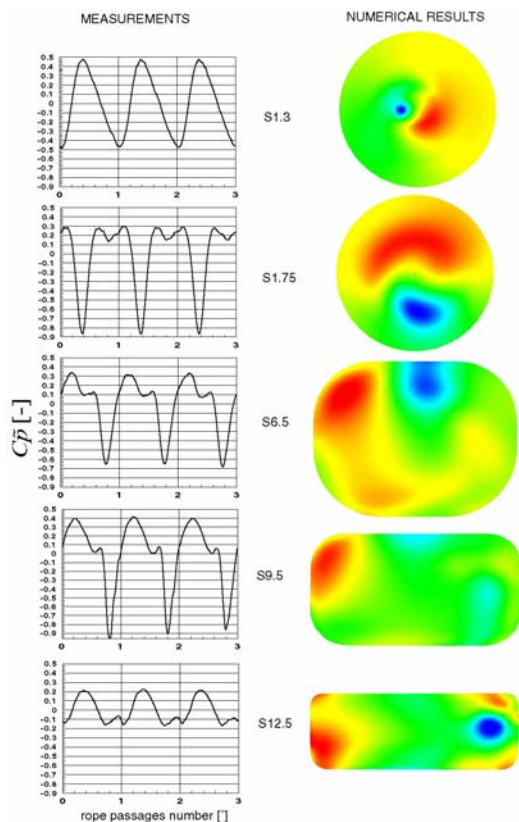


Fig. 12 Phase average at vortex frequency

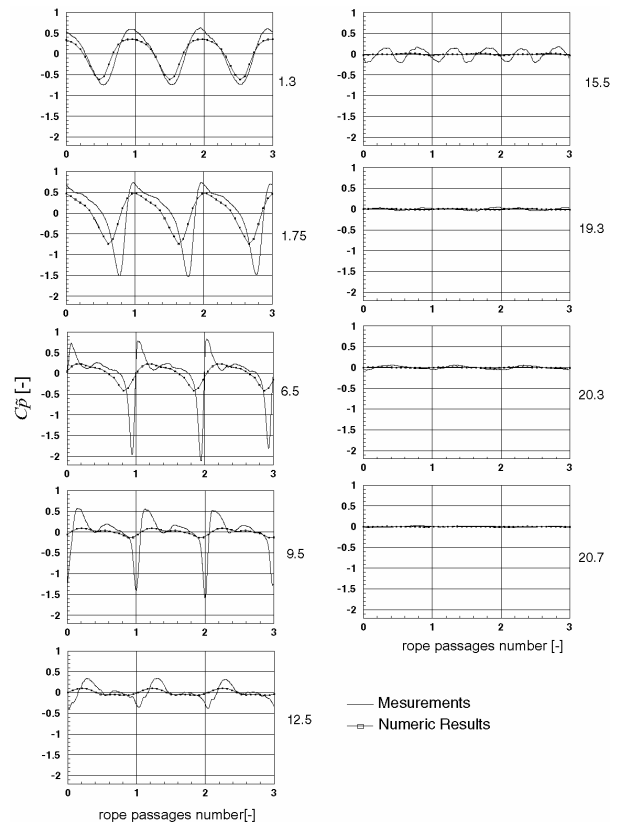


Fig. 13 Comparisons: measurements and calculation

The comparisons between the measurements and calculations, see Fig. 13, from the inlet to the outlet of the draft tube shown a good agreement for the 2 first sections, except for a slight

difference in the amplitudes and phase shift. The amplitude of the fluctuations given by the calculations decreases very fast in the elbow already at the section S6.5.

The representation of the phase of the wall pressure fluctuations at the vortex frequency, see Fig. 14, show how this fluctuations travel in the cone and elbow of the draft tube. This is a wave front that travels in a diagonal direction due to the swirling flow produced by the vortex rotation. At the inlet of the channels of the draft tube the swirl decays and a propagation of the pressure in a certain direction in the right channel is observed. In the left channel the direction of the propagation is not clear.

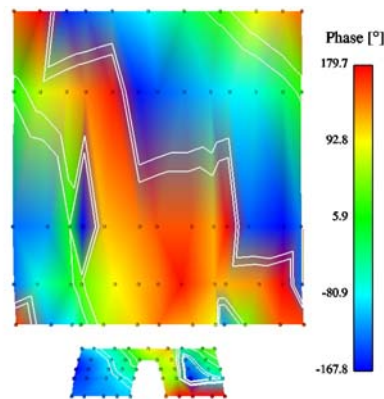


Fig. 14 Phase of the wall pressure fluctuations at vortex frequency

CONCLUSION

The analysis of the steady and unsteady pressure field is presented. 2 cases are studied: the first case concerning the operating points around the BEP and the second case regarding an operating point at low discharge without vapor phase. In the first case, the evolution of the pressure field in the whole draft tube go in the direction of the Mauri's calculation conclusions concerning the pressure recovery break-off, a vortex appears at the right channel, leading to an obstruction of this channel and to an increase of the draft tube global losses. The rotating component at f^* and the synchronous component at $20f^*$ of the pressure fluctuation field in the cone is pointed out. The influence of the spiral casing tongue on the pressure fluctuations field is also observed. The analysis of the low discharge operating point show the pressure fluctuation field at the vortex frequency and the wave front that travels in a diagonal direction due to the swiling flow produced by the vortex rotation. A good agreement is found between the measurements and the low discharge calculations by Mauri.

ACKNOWLEDGEMENT

We would like to thank the partners of the FLINDT Project (Eureka 1625) for their financial support and the staff of the LMH-EPFL for the technical support. We also would like to thank Dr. M. Farhat, Dr. G. Ciocan, Dr. S. Mauri for their contribution to the results analysis of this work.

REFERENCES

- Ref. 1 Avellan F., 2000, "Flow Investigation In A Francis Draft Tube: The Flindt Project", Proceedings of the Hydraulic Machinery and Systems 20th I.A.H.R. Symposium, 7-9 August, 2000, Charlotte, vol.1, Session DES, paper DES-11,12 pages.
- Ref. 2 Mauri S., 2002, "Numerical Simulation and Flow Analysis of an elbow diffuser", EPFL Thesis work, Laboratory for Hydraulic Machines, EPFL, Lausanne, Suisse.
- Ref. 3 Ciocan G. ,Mauri S.,Arpe J., Kueny J.L. ,2001 "Etude du Champ Instationnaire de Vitesse en Sortie de Roue de Turbine. Etude Expérimentale et Numérique". Publié dans : La Houille Blanche vol. 56, no 2, 2001 , Lausanne : IMHEF/EPFL, 2001
- Ref. 4 Nishi M., Yoshida K., Ma Z., Fujii M. "Alleviation of the Pressure Surge Observed in an Elbow Draft Tube by Installation of Fin". Proceedings of 20th IAHR Symposium on Hydraulic Machinery and Systems, 7-9 August, 2000, Charlotte..
- Ref. 5 Nishi M., Matsunaga S., Okamoto M., Takatsu K. "Wall Pressure Measurements as a Diagnosis of Draft Tube Surge", IAHR symposium, Belgrade, 1990.
- Ref. 6 Shi Qinghua. "Experimental Investigation of Frequency Characteristics of Draft Tube Pressure Pulsations for Francis Turbines". Proceedings of 18th IAHR Symposium on Hydraulic Machinery and Cavitation, Valencia.
- Ref. 7 Pedrizzetti G., Angelico G. "Model for vortex rope dynamics in Francis turbine outlet". Proceedings of 18th IAHR Symposium on Hydraulic Machinery and Cavitation, Valencia.
- Ref. 8 Mauri S., Kueny J.L., Avellan F., 2000."Numerical Prediction of the Flow in a Turbine Draft Tube, Influence of the Boundary Conditions". Proceedings of the ASME 2000 Fluids Engineering Division, Summer Meeting, June 11-15, 2000, Boston, Paper FEDSM2000-11056, 7 pages.